AQUA
Water Infrastructure, Ecosystems and Society

 AQUA — Water Infrastructure, Ecosystems and Society Vol 73 No 9, 1801 doi: 10.2166/aqua.2024.089

Utilizing the ANFIS and teaching-learning-based optimization (TLBO) methods to predict the maximum depth of scouring at culvert outlets

Nazila Kardan* and Tohid Habibi
Department of Civil Engineering, Azarbaijan Shahid Madani University, Tabriz, Iran
*Corresponding author. E-mail: n.kardan@azaruniv.ac.ir

ABSTRACT

Excessive scouring at culvert outlets is a widespread issue that often leads to culvert failure. At present, there is an absence of a universally applicable model for accurately predicting the occurrence of local scouring at culvert outlets. In this paper, a comparison is made between the performance of existing empirical equations and the results obtained from two advanced methods: adaptive neuro-fuzzy inference system (ANFIS) and the teaching-learning-based optimization (TLBO). This paper presents the development of the TLBO method, based on the ANFIS approach, for simulating scouring at culvert outlets. The algorithms for supervised training are applied by utilizing data collected from published studies. The results illustrate that the ANFIS -TLBO model successfully predicts scouring depth at culvert outlets with higher accuracy in comparison to existing empirical formulas. Furthermore, the model exhibits a wider range of applicability, accommodating diverse conditions. By integrating the ANFIS approach and TLBO optimization, the model surpasses the limitations of traditional empirical equations, providing engineers with a more reliable tool for predicting scour depth at culvert outlets. Ultimately, it can be concluded that the hybrid ANFIS -TLBO is a robust approach for scour depth prediction downstream of culverts.

Key words: ANFIS, culvert, empirical equations, prediction, scour depth, TLBO

HIGHLIGHTS

- Current anticipation equations are compared with results obtained from two adaptive network-based fuzzy inference systems (ANFISs) and teaching-learning-based optimization (TLBO) methods.
- TLBO methods are based on the ANFIS method in the case of simulating scouring downstream of culvert outlets.
- The ANFIS–TLBO is capable of anticipating the scouring depth at culvert outlets with greater accuracy than the existing empirical formula.

GRAPHICAL ABSTRACT

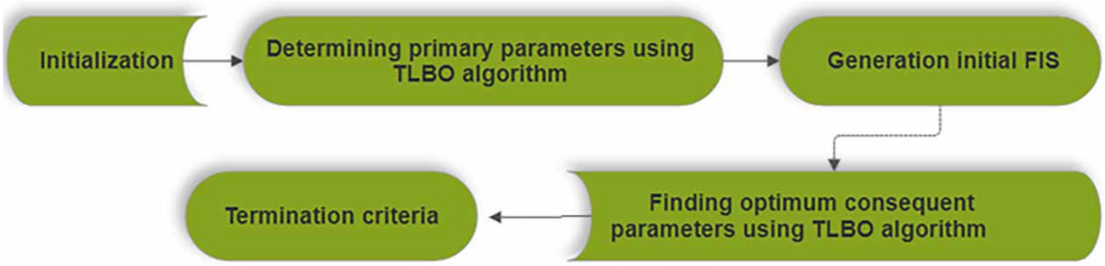

1. INTRODUCTION

Culverts are widely used hydraulic structures within water management systems to facilitate the conveyance of storm runoff beneath roadways, railways, and embankments (Sorourian *et al.* 2014). Furthermore, they can serve as bridge-like structures for vehicular transportation and contribute to the control and redirection of roadway runoff (Najafzadeh 2016). However, the design of culverts can occasionally give rise to issues, such as outlet scouring (Larry 2017). Scouring, particularly at the outlets of culverts, poses a significant threat to the structural integrity of culverts under both submerged and unsubmerged flow conditions. Therefore, it is imperative to implement effective countermeasures against scour to safeguard culverts. However, accurately estimating the development of scour depth at culvert outlets is equally crucial to avoid unnecessary overdesign and excessive project costs (Abida & Townsend 1991; Lim & Lim 1995).

Extensive studies have been conducted, resulting in a substantial accumulation of observations and recorded findings. Based on these findings, several analytical equations have been proposed, although their applicability is limited to specific data ranges (Abida & Townsend 1991; Lim 1995; Lim & Lim 1995; Ade & Rajaratnam 1998; Aderibigbe & Rajaratnam 1998; Liriano *et al.* 2002). In recent years, several studies have dedicated their focus to the implementation of optimization algorithms for the prediction of scouring depth at culvert outlets. These investigations have thoroughly examined the efficacy of various algorithms and conducted comparisons with traditional empirical equations to assess their performance.

An eminent study conducted by Hu *et al.* (2022) centered on the implementation of the particle swarm optimization (PSO) algorithm for the prediction of scouring depth at culvert outlets. The researchers extensively compared the performance of the PSO algorithm with traditional empirical equations and concluded that the PSO algorithm yielded more precise predictions. However, it is worth noting that the study did not undertake a comparative analysis of the PSO algorithm with other optimization methods or explore its performance concerning different culvert shapes. Zhang & Wu (2021) proposed a hybrid optimization algorithm that integrates the genetic algorithm (GA) and support vector regression to predict scouring depth at culvert outlets. The researchers demonstrated that the hybrid algorithm outperformed traditional empirical equations, leading to more accurate predictions. However, the study did not evaluate the algorithm's performance across different culvert shapes or compare it with other optimization methods. Li *et al.* (2022) conducted a recent study where they examined the application of the grey wolf optimizer (GWO) algorithm for predicting scouring depth at culvert outlets. The researchers compared the predictive performance of the GWO algorithm with traditional empirical equations and discovered that the GWO algorithm achieved higher accuracy in its predictions. However, similar to previous studies, the comparison was limited to empirical equations, and the study did not explore the algorithm's performance for different culvert shapes.

Previous research has provided evidence for the effectiveness of teaching-learning-based optimization (TLBO) in solving various optimization problems. For instance, Toğan (2012) utilized the TLBO method to optimize the design of planar steel frames and reported its superiority over alternative optimization algorithms such as GA, ant colony optimization, harmony search, and improved ant colony optimization algorithms (IACO). Roy *et al.* (2013) proposed an algorithm that integrates oppositional based learning with TLBO to effectively tackle hydrothermal short-term scheduling challenges. The results of their investigation displayed that TLBO outperformed other methods in terms of both convergence speed and solution quality. Ji *et al.* (2014) utilized the TLBO algorithm to optimize hyperparameters in order to predict short-term water demand using the least-squares support-vector machines (LS-SVM) algorithm. The results demonstrate that the tuned model using ATLBO achieves the highest regression accuracy, with a mean square error (MSE) of 280.75. The MSE for the forecasted values of the tuned LS-SVM model using TLBO is 626.07. Based on these findings, it can be concluded that ATLBO is the most effective approach for adjusting the hyperparameters of LS-SVM.

The examination yielded the absence of previous research that has delved into the utilization of the TLBO algorithm for the prediction of scouring depth at culvert outlets. The TLBO algorithm has exhibited promising performance in a multitude of optimization problems, and its simplicity and effectiveness position it as a well-suited candidate for this intended application.

The objective of this research is to develop and compare an optimized adaptive neuro-fuzzy inference system (ANFIS) model, utilizing the TLBO algorithm, with existing empirical equations for the prediction of scour depth at culvert outlets. The study aims to evaluate the predictive capabilities of these approaches for different culvert shapes using consistent experimental data. It is worth noting that the TLBO algorithm, which draws inspiration from the teaching and learning process, is a population-based meta-heuristic. In this algorithm, students learn from both instructors and peers, creating a unique learning mechanism. Furthermore, the TLBO algorithm does not necessitate intricate parameter tuning. Two distinct datasets, one for circular culverts and another for rectangular culverts, were utilized in this study to develop and validate a predictive model. The dataset provided by Sorourian *et al.* (2016) consisted of data pertaining to rectangular culverts, while the dataset by Opie (1968) contained detailed information on circular culverts. The optimization process of the predictive model involved the utilization of the ANFIS and the TLBO algorithm. In order to evaluate the performance of the optimized model, a comparison was made against both the standard ANFIS model and empirical equations. This evaluation was conducted by comparing the predicted scour depths with the measured scour depths, using error metrics as a means of assessment.

Culverts serve a vital function in the management of stormwater runoff beneath transportation infrastructure. Nonetheless, the occurrence of scouring at outlets presents significant structural risks. Precisely assessing the development of scour depth is of utmost importance to guarantee the integrity and prolonged lifespan of culverts. The primary goal of this research is to augment the existing comprehension and predictive abilities with the aim of informing design practices more effectively through the implementation of a groundbreaking optimization approach.

2. EXPERIMENTAL DATA AND INFLUENCING PARAMETERS

Figure 1 visually illustrates the key parameters that exert significant influence on the scouring depth.

Previous studies imply that the maximum scour depth downstream of the culverts is a function of incoming flow, flume configuration, and sediment properties (Azamathulla & Ghani 2010; Azamathulla & Haque 2012, 2013; Najafzadeh 2015; Najafzadeh & Kargar 2019):

$$d_{se} = f(d_\circ, b_\circ, \mu, \rho, U_\circ, H, B, d_{50}, \sigma_g, \rho_s) \tag{1}$$

where f denotes an unknown function. d_{se} is the maximum scour depth at equilibrium condition, $d_\circ$ is the diameter of a circular outlet or the brink water depth of noncircular outlets, $b_\circ$ is the base width of noncircular outlets, μ is the dynamic viscosity of water, ρ is the water density, $U_\circ$ is the mean velocity of the incoming flow, H is the tailwater depth, B is the width of the downstream channel, d_{50} is the median grain size, σ_g is the geometric standard deviation of the grain size distribution, and ρ_s is the grain density, Fr_d is the particle densimetric Froude number; $U_\circ/\sqrt{(\rho_s - \rho)gd_{50}}$. Then the dimensionless parameters were applied to develop the proposed models for predicting scour depth at culvert outlets. Equation (2) serves as the fundamental basis for these models, leveraging the utilization of dimensionless parameters:

$$\frac{d_{se}}{d_\circ} = f\left(Fr_d, \sigma_g, \frac{H}{d_\circ}, \frac{b_\circ}{d_\circ}, \frac{d_{50}}{d_\circ}\right) \tag{2}$$

The dataset employed in this study was compiled from various published sources (Opie 1968; Bohan 1970; Rajaratnam & Berry 1977; Rajaratnam 1981; Ruff *et al.* 1982; Rajaratnam & MacDougall 1983; Ali & Lim 1986; Abida & Townsend 1991; Ade & Rajaratnam 1998; Aderibigbe & Rajaratnam 1998; Liriano 1999; Liriano & Dey 2001; Sorourian *et al.* 2016). A total of 201 datasets were utilized for circular culverts, while 151 datasets were employed for rectangular culverts.

To ensure the integrity of the data, any experimental data that exhibited illogical or implausible scouring depth values were omitted from the analysis. This step was taken to maintain the accuracy and reliability of the dataset used for evaluating the performance of the ANFIS–TLBO model and comparing it with existing empirical equations. The dataset primarily consisted of uniform sands with a median grain size (d_{50}) ranging from 0.38 to 29 mm. The diameter of circular culvert outlets (d_0) ranged from 2.54 to 311 mm, while the height of rectangular culvert outlets varied accordingly. The submergence ratio varied from 0.25 to 124, encompassing a wide range of hydraulic conditions. In addition, the flow velocity at the culvert outlets ranged from 0.747 to 11.176 m/s. Additional information regarding the dataset can be found in Table 1 for circular culverts and Table 2 for rectangular culverts. These tables offer a comprehensive overview of the data employed in this study.

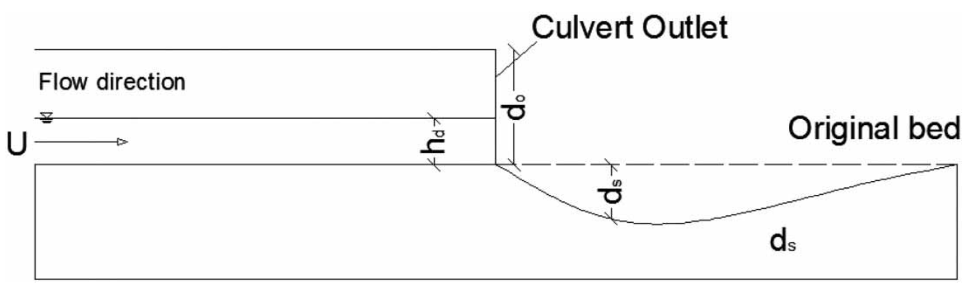

Figure 1 | Factors influencing the depth of scour at culvert outlets.

Table 1 | Experimental data utilized for circular culverts

	Notation	Parameters	Min.	Max.	Ave.	St. deviation
Outlet diameter (mm)	d_0	x_1	2.54	311	111.5	46.20
Velocity (m/s)	U	x_2	0.747	11.176	5.34	2.12
Sediment size (mm)	D_{50}	x_3	0.38	29	7.95	8.11
Depth of flow/outlet diameter	h_d/d_0	x_4	0	29.76	5.67	2.39
Tailwater depth	h_t/d_0	x_5	0.4	36	10.49	4.78
Submergence depth	h_u/d_0	x_6	0.25	124	41.05	15.28
Scour depth (m)	d_s	y	0.03	1.07	0.36	0.157

Table 2 | Experimental data utilized for rectangular culverts

	Notation	Parameters	Min.	Max.	Ave.	St. Deviation
Outlet diameter (mm)	d_0	x_1	2.54	285	83.52	42.31
Velocity (m/s)	U	x_2	0.568	12.15	4.59	2.83
Sediment size (mm)	D_{50}	x_3	0.42	32	8.19	10.75
Depth of flow/Outlet diameter	h_d/d_0	x_4	0	25.38	6.67	3.06
Tailwater depth	h_t/d_0	x_5	0.5	48	13.10	5.99
Submergence depth	h_u/d_0	x_6	0.25	218	62.37	22.14
Scour depth (m)	d_s	y	0.03	0.59	0.18	0.11

3. CATEGORIZING EQUATIONS

In two distinct cross-sections of culverts, namely circular and square shapes, significant variations in flow patterns were observed, resulting in different scouring phenomena. Consequently, the scouring process and depth differ between these two sections.

In the case of circular section culverts, the flow pattern is typically characterized by a smooth and streamlined flow. The circular shape facilitates a more uniform distribution of velocity, which in turn promotes a stable flow pattern. This feature helps mitigate the formation of turbulence and eddies, ultimately reducing the potential for scouring. On the other hand, square-section culverts can exhibit a more complex flow pattern. The corners and edges inherent in the square shape (known as lateral contractions) can cause flow irregularities, leading to the generation of turbulence and vortices. These flow disturbances significantly increase the likelihood of scouring by creating localized areas of high velocity and pressure fluctuations.

In the case of circular section culverts, the smooth flow pattern aids in reducing the potential for scour. The circular shape facilitates a more uniform distribution of flow energy, effectively minimizing localized erosion. However, it is important to note that scouring can still occur downstream of the culvert outlet due to a phenomenon known as the hydraulic jump. On the other hand, square-section culverts experience flow irregularities and the presence of flow jets, which can result in higher flow velocities and increased turbulence. These factors contribute to a higher likelihood of scouring. The corners and edges characteristic of the square shape create areas of concentrated flow and pressure differentials, which can lead to scouring at the culvert inlet and outlet, as well as along the sidewalls.

Table 3 presents a comprehensive summary of the empirical equations, featuring seven equations categorized under Group A for rectangular culverts, and an additional seven equations classified under Group B for circular culverts. These traditional equations have challenges in adequately addressing the scale impact, which refers to the difficulty of accurately predicting outcomes when extrapolating from small-scale laboratory datasets to larger real-world scenarios. Artificial intelligence (AI) methodologies, including machine learning algorithms, also rely on training data, which may include small-scale laboratory datasets. While it is true that AI methodologies may encounter similar limitations, it is important to note that these

Table 3 | Selected equations for circular and rectangular culverts

Group		No.	Authors	Equations
A	Rectangular	1	Schoklitsch (1937)	$d_s = kd_{90}^{-0.32}h_c^{0.2}q^{0.57}$
		2	Laursen (1963)	$\frac{d_s}{h_u} = 0.13\left[\frac{Q}{d_{50}^{\frac{1}{3}}h_u^{\frac{7}{6}}B}\right]^{\frac{8}{7}} - 1$
		3	Valentin (1967)	$\frac{d_s}{h_d} = \left(\exp\frac{F_r - 2}{2.03}\right)\left(\frac{d_{90}}{h_d}\right)^{-0.55}$
		4	Chen (1970)	$\frac{d_s}{H} = \left(\exp\frac{F_r - 2}{2.03} - 0.373\right)\left(\frac{d_{90}}{H}\right)^{-0.50}$
		5	Abida & Townsend (1991)	$\frac{d_s}{H} = \left(\exp\frac{F_r - 2}{2.03} - 0.373\right)\left(\frac{d_{50}}{H}\right)^{-0.275}$
		6	Kerenyi *et al.* (2007)	$d_s = 2.2658\left[\frac{Qh_u}{6.19h_uBd_{50}^{\frac{1}{3}}}\right]^{\frac{6}{7}}$
		7	Sorourian *et al.* (2015)	$\frac{d_{sm}}{h_d} = 0.27F_d + 0.29B - 0.35$
B	Circular	1	Abt *et al.* (1984)	$\frac{d_s}{d_\circ} = -3.67(F_d^{0.57}d_{50}^{0.4}\sigma_g^{-0.4})$
		2	Lim & Lim (1995)	$\frac{d_s}{d_\circ} = 0.45F_d$
		3	Liriano (1999)	$\frac{d_s}{d_\circ} = a\ln(F_d) + b$
		4	Sarathi *et al.* (2008)	$\frac{d_{sm}}{d_\circ} = a\ln(F_d - b) \qquad 0.5 \le \frac{h_t}{d_\circ} \le 3$ $a = -0.66\frac{h_t}{d_\circ} + 2.34$ $b = 1.31\frac{h_t}{d_\circ} - 1.73$
		5	Emami & Schleiss (2010)	$\frac{d_{sm}}{d_\circ} = a\ln(F_d)$ $a = -0.6\frac{h_t}{d_\circ} + 1.80$ $b = 1.23\frac{h_t}{d_\circ} - 2.25$
		6	Azamathulla & Haque (2012)	$\frac{d_s}{d_\circ} = \left[\frac{-6.62 + F_d}{\frac{\sqrt{F_d}}{\frac{H}{d_\circ}} + \frac{9.65}{\sigma_g}}\right] + \left[\frac{d_{50}}{d_\circ} - \frac{\frac{H}{d_\circ}}{e^{[2.34+(d_{50}/d_\circ)]} + e^{\sigma_g}}\right] + \left(F_d\sqrt{\sigma_g\frac{H}{d_\circ}}\right)^{0.5}$

methodologies have the potential to mitigate the scale impact issue in a few ways; feature representation, transfer learning, ensemble methods, and data augmentation.

4. THE PROPOSED HYBRID AI MODELS

Recently, there has been a significant advancement in computational modeling approaches (Yaseen *et al.* 2018a). This is attributed to their capacity to effectively tackle complex problems characterized by high levels of nonlinearity, non-stationarity, and stochasticity (Yaseen *et al.* 2015). In recent times, there has been a notable expansion of hybridized AI models integrated with global optimization algorithms (Ghorbani *et al.* 2017). Among the various optimization methodologies, nature-inspired bio-algorithms have demonstrated their efficacy by providing robust and reliable solutions for the hyperparameters of AI models (Maier *et al.* 2014). This is done with the aim of enhancing the cohesive learning mechanism of computational models to accurately approximate the desired solution. In the present investigation, the TLBO algorithm is integrated with the ANFIS model to estimate the maximum scour depth downstream of a culvert. Culvert scouring is a widely recognized and intricate problem in the field of hydraulic and highway engineering. Hence, the proposal of hybridized AI models aims to develop a reliable and accurate predictive model for determining the scour depth.

4.1. Classical ANFIS model

The ANFIS is a multilayer feed-forward network that incorporates principles of fuzzy logic to effectively model complex relationships between input and output variables (Jang 1993). In the ANFIS architecture, each node in the network performs a specific function on the incoming signals and is associated with a set of parameters. These parameters are dynamically adjusted during the learning process to optimize the network's performance.

Figure 2 illustrates the ANFIS architecture, which encompasses five layers: the fuzzify layer, the rule layer, the normalized layer, the defuzzify layer, and the output layer (Abraham 2005). Notably, nodes within layers 2, 3, and 5 are regarded as fixed, indicating that their parameters remain constant throughout the learning process. In contrast, the nodes in layers 1 and 4 are adaptive nodes, and their parameters are adjusted based on the training data. To illustrate the functionality of ANFIS, x is equal to A_1 and y is equal to B_1. In this case, the ANFIS model applies the first equation to evaluate the output. The specific mathematical form of this equation depends on the defined rules and membership functions in the ANFIS model.

It is important to note that ANFIS has the ability to learn from previous outcomes and establish connections between inputs and visible outputs by adapting its parameters based on the training data. This adaptive capability enables ANFIS to proficiently model intricate relationships and generate precise predictions. The ANFIS rules are presented mathematically as follows:

$$f = p_1x + q_1y + r_1 \tag{3}$$

Moreover, if the value of x is equal to the square of A (A_2) and the value of y is equal to the square of B (B_2), the third equation can be rewritten as follows:

$$f = p_2x + q_2y + r_2 \tag{4}$$

where x and y represent the input variables, (A_1 and A_2) and (B_1 and B_2) are the membership functions for the input x and the input y, respectively, f represents the output, and p, q, and r denote the design parameters determined during the learning process of ANFIS.

The distinct layers of this network serve specific purposes and possess unique applications. Each node I in the first layer is associated with a membership function that represents its distinct application:

$$\begin{aligned} O_{1,i} &= \sigma_{A_{i(x)}} \\ O_{1,i} &= \sigma_{B_{i(x)}} \end{aligned} \tag{5}$$

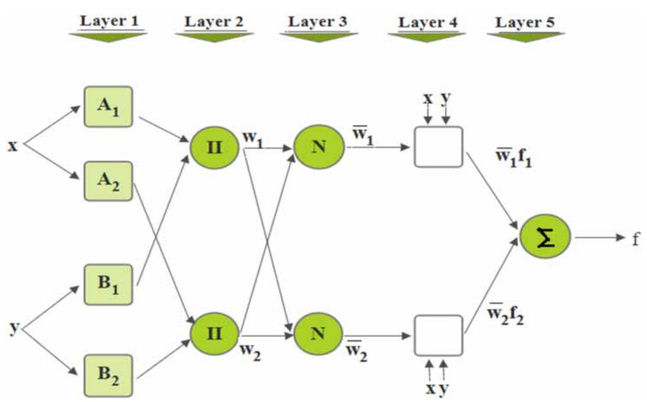

Figure 2 | Conceptual graph of the ANFIS model.

In Equation (5), A_i denotes the linguistic variable, x denotes the input node i, and $O_{1,i}$ denotes the membership function A_i. Typically, A_i is defined by employing the Gaussian function, as shown below:

$$\sigma_{A_{i(x)}} = \exp\left(\frac{-(x-c)^2}{\sigma^2}\right) \tag{6}$$

The center of the Gaussian membership function mentioned earlier is denoted as c, while the standard deviation σ is defined accordingly. The calculation of the firing strength in the second layer follows the rule described below:

$$\omega_i = \sigma_{A_{i(x)}} \times \sigma_{B_{i(x)}} \qquad i = 1, 2, \ \ldots . \tag{7}$$

The third layer employs the following mathematical formula to regulate the firing strength associated with each rule:

$$\bar{\omega} = \frac{\omega_i}{\omega_1 + \omega_2} \tag{8}$$

Within the fourth layer, the set of fuzzy rules is obtained through the following process of derivation:

$$\bar{\omega}_i f_i = \bar{\omega}_i (p_i x + q_i y + r_i) \tag{9}$$

This layer, known as the fourth layer, is responsible for combining the fuzzy sets and their associated membership functions to calculate the rule firing strengths. The specific implementation and mathematical operations used in the rule layer can vary, allowing for flexibility in the ANFIS architecture.

Within the fifth layer, the individual outcomes generated in the fourth layer are amalgamated and integrated. This integration process involves aggregating the outputs from the fuzzy rules to obtain the final outcome. Through the aggregation of results from multiple rules, the network adeptly captures and synthesizes collective information, enabling it to reach a final inference or decision based on the given input variables (Equation (10)). This integration step within the fifth layer plays a pivotal role in producing a comprehensive and definitive output for the ANFIS network:

$$\sum_i \bar{\omega}_i f_i = \frac{\sum_i \omega_i f_i}{\sum_i \omega_i} \tag{10}$$

4.2. Teaching and learning-based optimization algorithm (TLBO)

Rao *et al.* (2011) presented the TLBO algorithm, a meta-heuristic methodology rooted in natural phenomena. TLBO draws inspiration from the educational dynamics of a classroom, where students engage in iterative learning and practice, benefiting from both the guidance of their instructor and interaction with their peers.

The TLBO algorithm is composed of two distinct phases. In the initial phase, the learners, representing the individuals in the population, undergo training guided by the teacher. The teacher, selected based on their optimal fitness score, assumes a pivotal role in instructing the learners. Subsequently, in the second phase, the learners engage in knowledge acquisition and information exchange with their peers, further enriching their learning process. Similar to other meta-heuristic algorithms TLBO employs a primary population of individuals called 'learners.' The fitness function is assessed for each learner and the individual with the highest fitness score is designated as the teacher.

In the TLBO framework, the optimization problem's design parameters are treated as instructional materials provided to the students. The primary objective of the algorithm is to optimize these design parameters by selecting values that maximize the response of the objective function. The fitness function serves as a metric to gauge the level of learning accomplished by the students (Hassanzadeh *et al.* 2019).

4.2.1. Teacher phase

During this phase, the teacher assumes a vital role in imparting knowledge to the students, emulating an authentic classroom context. The aim is to augment the students' knowledge and elevate it to the level of the teacher. However, practical limitations such as scarce educational resources, disparities in student aptitude, and constrained preparation time may impede the attainment of uniform learning outcomes among students. Consequently, the teacher endeavors to enhance the overall average knowledge level to a distinguished standard of scientific proficiency.

In Equation (11), during each iteration i, 'n' ($k = 1, 2,..., n$) represents the quantity of individuals in the primary population. 'm' signifies the count of design variables ($j = (1, 2,..., m)$). '$M_{j,i}$' denotes the average value of the 'j' variable in the initial population (class). Within the set of all design variables, the optimal solution in the population is represented as $X_{\text{total-kbest},i}$. The process of selecting the teacher adheres to the algorithm guidelines, wherein the teacher is chosen based on their expertise in identifying the most promising learners among the population.

After the completion of the teacher's role, the average progress level of each student in every subject is determined utilizing the equation provided in the research conducted by Azamathulla *et al.* (2008):

$$\text{Difference mean}_{j,k,i} = r_i(X_{j,k_{\text{best}},i} - T_F M_{j,i}) \tag{11}$$

The random coefficient, r_i, is a value between 0 and 1. $X_{\text{j,kbest},i}$ represents the achievement of the highest-performing student in the subject, while T_F is the coefficient that quantifies the impact of the teacher on the teaching process. The value of T_F is determined by means of the following equation:

$$T_F = \text{round}\ [1 + \text{rand}(0, 1)\{1 - 2\}] \tag{12}$$

The degree of randomness in the teaching factor (T_F) is determined by Equation (12) and integrated into the algorithm. Several studies conducted by Rao *et al.* (2011) demonstrate that the optimal value for the teacher coefficient is either 1 or 2, as computed by Equation (12). Based on the values derived from Equation (11), the responses at each iteration are determined using the following equation for the difference mean$_{j,k,i}$:

$$X^*_{j,k,i} = X_{j,k,k} + \text{Difference mean}_{j,k,i} T_F = \text{round}[1 + \text{rand}(0, 1)\{1 - 2\}] \tag{13}$$

During this phase, the algorithm computes a new conclusion, $X^*{}_{*j,k,i}$, which is only accepted if it demonstrates an improvement. At the conclusion of this phase, the acquired results are gathered and utilized as inputs for the subsequent phase, encompassing all individuals in the population and variables.

In TLBO, the teacher value represents the best solution found during the optimization process. The estimation of the optimum teacher value depends on the specific problem and objective function. During the initialization phase, the teacher value is set to a random solution within the search space. As the TLBO algorithm iterates, new solutions are generated and evaluated. If a newly generated solution is better than the current teacher value, it is updated as the optimal solution. The TLBO algorithm keeps track of the best solution attained so far, updating the teacher value whenever a fitter solution is found.

4.2.2. Learners' phase

The second phase of the TLBO algorithm is commonly referred to as the students' phase. During this phase, the students engage in random communication and knowledge exchange with one another. This facilitates the transfer of knowledge from one student with a higher level of expertise to another student. If two students, A and B, possess different levels of knowledge, it is assumed that the student with greater knowledge will transfer his or her knowledge to the other student, as described by the following equation.

This phase simulates the notion of knowledge exchange within a simulated classroom scenario, where students engage in interactive collaboration to learn from each other. By incorporating this aspect into the algorithm, the TLBO algorithm harnesses the collective intelligence of the population to enhance the learning process and optimize the overall performance of the algorithm:

$$\begin{aligned} X^{**}_{j,A,i} &= X^*_{j,A,i} + r_i(X^*_{j,A,i} - X^*_{j,B,i}) \quad \text{if} \quad X^*_{\text{total}-A,i} < X^*_{\text{total}-B,i} \\ X^{**}_{j,A,i} &= X^*_{j,A,i} + r_i(X^*_{j,B,i} - X^*_{j,A,i}) \quad \text{if} \quad X^*_{\text{total}-B,i} < X^*_{\text{total}-A,i} \end{aligned} \tag{14}$$

In scenarios where the objective is to maximize rather than minimize, the previously mentioned equations undergo necessary modifications. These adjustments are implemented to ensure the algorithm aligns with the goal of maximizing the outcome. The specific adaptations made to the equations are contingent upon the algorithm's nature and the specific context in which it is implemented. By customizing the equations to suit the desired maximum outcome, the algorithm can effectively optimize and attain the intended objectives:

$$\begin{aligned} X^{**}_{j,A,i} &= X^{*}_{j,A,i} + r_i(X^{*}_{j,A,i} - X^{*}_{j,B,i}) \quad \text{if} \quad X^{*}_{\text{total}-B,i} < X^{*}_{\text{total}-A,i} \\ X^{**}_{j,A,i} &= X^{*}_{j,A,i} + r_i(X^{*}_{j,B,i} - X^{*}_{j,A,i}) \quad \text{if} \quad X^{*}_{\text{total}-A,i} < X^{*}_{\text{total}-B,i} \end{aligned} \tag{15}$$

In Figure 3, the implementation process of the algorithm is presented. An eminent benefit of this approach, in contradistinction to alternative evolutionary optimization algorithms, lies in its nondependence on algorithm-specific parameters. Essentially, apart from specifying the initial population size and the number of generations, this algorithm does not necessitate any additional specific parameters. This sets it apart from numerous other algorithms that heavily rely on multiple parameters, the modification of which can detrimentally affect their effectiveness. The absence of algorithm-specific parameters facilitates the implementation and diminishes the likelihood of suboptimal performance.

Several studies have compared the TLBO algorithm with other popular optimization algorithms such as GA and PSO. TLBO has demonstrated promising results in various applications and outperformed GA and PSO in terms of solution quality and convergence speed for the economic load dispatch problem. However, it is important to consider that algorithm performance may vary based on the specific problem and parameter settings. Conducting a tailored comparative study or benchmarking analysis is recommended to determine the most suitable algorithm for a given optimization task, considering the problem's characteristics.

4.3. Hybrid model parameters

The TLBO optimization technique is utilized to determine the ANFIS parameters. One advantage of the TLBO algorithm is that it does not require any algorithm-specific parameters. The control parameters of the final algorithm are thus limited to the number of iterations and population size, making it convenient for immediate application without the need for parameter tuning. In this study, the initial parameters in Equation (7), specifically ω_i, σ_i, and c_i, are optimized using the TLBO algorithm. Moreover, the optimization process also involves training the membership function-related parameters (p_i, q_i, r_i) mentioned in Equation (9). The TLBO algorithm is utilized to estimate the weight parameter w_{i}, which corresponds to the maximum scouring depth downstream culverts. Initially, random search spaces are generated for the ANFIS parameters to accomplish this objective. Subsequently, these parameters are adjusted using the TLBO algorithm. This iterative process continues until a specified stopping condition is met. By incorporating the TLBO algorithm into the ANFIS approach, the optimization process is strengthened, enabling the discovery of more robust solutions. This integration effectively mitigates the limitations associated with gradient-based methods and significantly enhances the overall effectiveness of the model. The parameter setting of the TLBO algorithm is presented in Table 4.

4.4. *k*-Fold cross-validation

Cross-validation is a valuable technique utilized to assess the performance of prediction models on independent datasets. It enables an unbiased evaluation of the model's predictive power without introducing any form of bias in the predictions. The general process encompasses the random partitioning of the dataset into multiple equivalent subsets (folds), followed by the

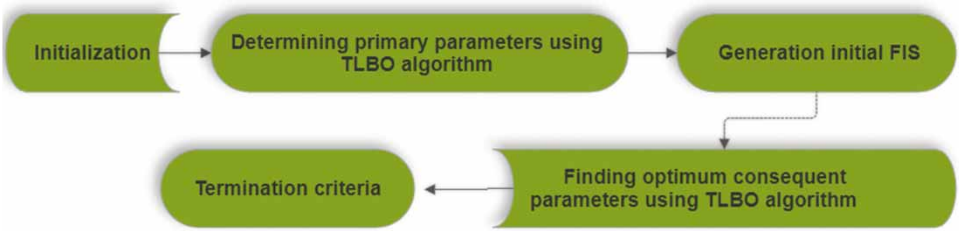

Figure 3 | Proposed integrated ANFIS model with evolutionary optimization algorithms.

Table 4 | Parameter setting of employed evolutionary algorithms

Evolutionary algorithm	Parameter description	Parameter value
ANFIS	Train epoch	200
	Train-error goal	0
	Train-initial step size	0.01
	Train-step size decrease	0.9
	Train-step size increase	1.1
TLBO	Population size	60
	Maximum iteration number	400

iterative construction and evaluation of predictive models. During each iteration, a single subset is designated for testing the model, while the remaining subsets are utilized for training. This methodology is widely referred to as '*k*-fold cross-validation', where *k* represents the number of folds. Figure 4 visually depicts a five-fold cross-validation scenario.

In this study, the collected data is divided randomly into five subsets, and the process of model training and evaluation is repeated five times. By adhering to the aforementioned approach, a significant portion of the available data is employed for training the models, while the remaining 20% is designated for testing and assessing their performance. To investigate the robustness of the models and their reliance on the selected data, the five-fold cross-validation is executed twice. This methodology effectively addresses concerns such as overfitting and provides valuable insights into the models' generalizability to independent datasets. The effectiveness and suitability of the proposed models are assessed utilizing the *k*-fold cross-validation approach and performance metrics, including root mean square error (RMSE), R^2, mean absolute error (MAE), and mean absolute percentage error (MAPE). By employing this rigorous cross-validation methodology, the study ensures a comprehensive evaluation of the models and provides an in-depth assessment of their performance.

The dataset consisted of 201 data points for circular-shaped culverts and 151 data points for rectangular ones. These were divided into five subsets, with 40 data points for circular shape culverts and 30 data points for rectangular ones in each fold.

The choice of '*k*' in *k*-fold cross-validation depends on factors like dataset size and model complexity. A common value is 5, where the dataset is divided into five folds. Each fold is used once as a validation set, while the others are used for training the model. Similar characteristics across subsets are recommended. Having a sufficient number of data points in each fold is important for meaningful model evaluation. Aim for roughly equal numbers in each fold if possible. If the dataset is small, alternative methods like leave-one-out cross-validation can be considered for more reliable evaluation. It is essential to have an equal distribution of data points across folds for meaningful model evaluation in *k*-fold cross-validation.

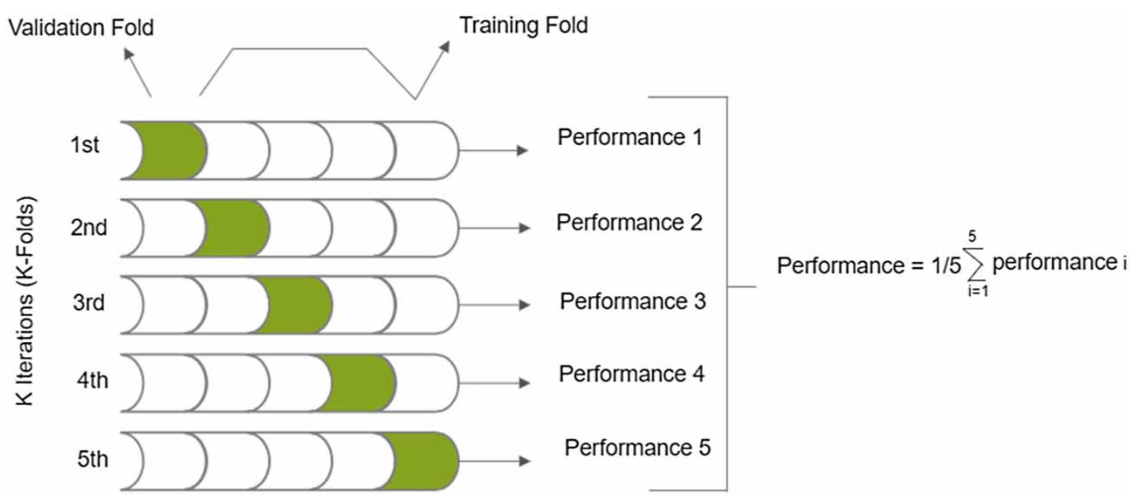

Figure 4 | Evaluation of model performance through five-fold cross-validation.

5. CRITERIA FOR ERROR FUNCTIONS

To evaluate the effectiveness of hybrid predictive models in forecasting the maximum scour depth caused by a horizontal jet downstream of culverts during both training and testing phases, error indices including RMSE, R^2, MAE, and MAPE were utilized (Yaseen *et al.* 2018a, 2018b; Abdulelah Al-Sudani *et al.* 2019; Sharafati *et al.* 2019; Sharafati *et al.* 2020a, 2020b, 2020c).

These functions are formally defined in Equation (16). The disparity between the ANFIS outputs and the target values is computed to enhance the optimization process of TLBO:

$$
\begin{aligned}
\mathrm{RMSE} &= \sqrt{\frac{1}{N}\sum_{i=1}^{N}\left(\left(\frac{d_{se}}{d_\circ}\right)_{\mathrm{obs},i}-\left(\frac{d_{se}}{d_\circ}\right)_{\mathrm{sim},i}\right)^2}\\
R^2 &= 1-\frac{\sum_{i=1}^{N}\left(\left(\frac{d_{se}}{d_\circ}\right)_{\mathrm{obs},i}-\left(\frac{d_{se}}{d_\circ}\right)_{\mathrm{sim},i}\right)^2}{\sum_{i=1}^{N}\left(\left(\frac{d_{se}}{d_\circ}\right)_{\mathrm{sim},i}-\overline{\left(\frac{d_{se}}{d_\circ}\right)}_{\mathrm{sim}}\right)^2}\\
\mathrm{MAE} &= \frac{1}{N}\sum_{i=1}^{N}\left|\left(\left(\frac{d_{se}}{d_\circ}\right)_{\mathrm{obs},i}-\left(\frac{d_{se}}{d_\circ}\right)_{\mathrm{sim},i}\right)\right|\\
\mathrm{MAPE} &= \frac{100}{N}\times\sum_{i=1}^{N}\left|\frac{\left(\left(\frac{d_{se}}{d_\circ}\right)_{\mathrm{obs},i}-\left(\frac{d_{se}}{d_\circ}\right)_{\mathrm{sim},i}\right)}{\left(\frac{d_{se}}{d_\circ}\right)_{\mathrm{obs},i}}\right|
\end{aligned}
\tag{16}
$$

where the $(d_{se}/d_\circ)_{\mathrm{obs},i}$ and $(d_{se}/d_\circ)_{\mathrm{sim},i}$ are the ith observed and predicted nondimensional scour depth magnitudes, $\left(\overline{d_{se}/d_\circ}\right)_{\mathrm{sim}}$ denote the predicted mean magnitudes of the nondimensional scour depth. N is the number of datasets. Optimal model performance is indicated by lower values of RMSE, MAPE, and MAE, while higher values of R^2 suggest a stronger correspondence between the model's predictions and the observed values.

6. RESULTS AND DISCUSSION

6.1. Results of the proposed model (ANFIS–TLBO)

The study investigated the feasibility and efficacy of the proposed model in accurately predicting culvert outlet scour in circular and rectangular cross-sections. The evaluation function's outcomes were utilized as a benchmark and compared to the results obtained from standard ANFIS and empirical equations.

Tables 5 and 6 illustrate the impact of the proposed model on the cross-fold modeling performance for both circular and rectangular culverts. The results of both datasets indicate that superior outcomes were achieved with the proposed model in circular culverts, as evidenced by Figures 5 and 6. For example, the MAPE decreased by 38.6%, and the determination coefficient in the laboratory dataset increased by 5.5% relative to the field dataset. The analysis of the outcomes from both datasets

Table 5 | ANFIS–TLBO model results for circular culverts dataset in 10 independent runs

	ANFIS–TLBO	1	2	3	4	5	6	7	8	9	10	Ave.	St. deviation
Train	R^2	0.932	0.930	0.911	0.909	0.902	.881	0.899	0.905	0.895	0.918	0.901	0.032
	MAPE (%)	23.2	52.2	22.5	28.3	24.6	23.9	41.1	31.8	21.9	22.7	46.5	23.7
	RMSE (mm)	188	203	234	309	195	186	216	183	198	234	209	7.8
	MAE (mm)	83	101	123	136	81	85	93	92	109	138	122	5.9
Test	R^2	.824	.856	.898	.836	.879	.835	.845	.852	.817	.847	.883	0.045
	MAPE (%)	31.2	28.9	67.2	35.6	22.9	28.7	25.4	33.6	24.4	24.0	33.5	22.8
	RMSE (mm)	223	289	284	256	221	237	229	198	242	231	226	6.4
	MAE (mm)	116	155	172	139	165	129	158	153	168	129	154	4.4

Table 6 | ANFIS–TLBO model results for rectangular culverts dataset in 10 independent runs

	ANFIS–TLBO	1	2	3	4	5	6	7	8	9	10	Ave.	St. deviation
Train	R^2	0.878	0.883	0.891	0.865	0.887	0.901	0.913	0.886	0.867	0.903	0.875	0.042
	MAPE (%)	31.2	33.9	22.8	21.9	18.9	48.9	31.8	65.7	25.3	32.3	33.8	18.2
	RMSE (mm)	32.2	31.9	33.6	32.7	31.3	28.9	33.3	29.8	33.8	31.5	31.4	3.1
	MAE (mm)	23.2	22.9	22.6	22.1	24.5	22.6	23.8	22.2	24.3	21.8	22.5	1.5
Test	R^2	0.812	0.789	.823	.836	.845	.817	.869	.880	.819	0.756	0.825	0.046
	MAPE (%)	18.9	41.3	22.2	25.6	18.2	26.7	19.2	33.5	21.8	21.3	25.9	16.9
	RMSE (mm)	29.6	33.5	29.4	28.7	30.1	32.2	33.6	31.8	32.5	34.8	30.4	2.6
	MAE (mm)	25.3	24.8	26.2	26.8	24.7	24.5	25.6	25.5	26.7	24.5	25.2	1.8

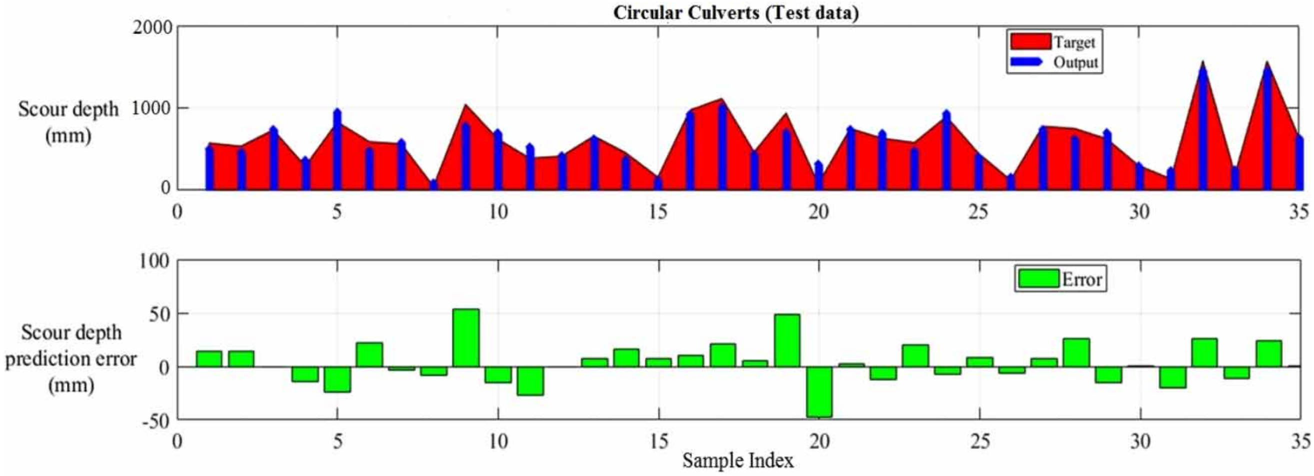

Figure 5 | Comparison of observed and predicted scour data for the best testing fold of circular culverts using the proposed model.

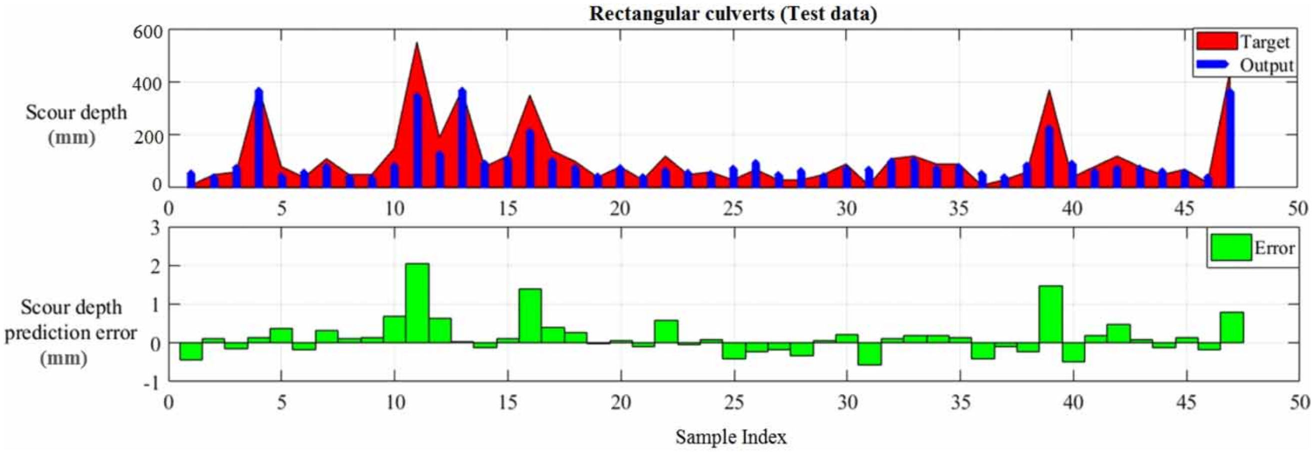

Figure 6 | Comparison of observed and predicted scour data for the best testing fold of rectangular culverts using the proposed model.

indicates that the proposed model demonstrates a high level of strength and reliability, as the output for both training and testing data exhibits remarkable similarity.

For instance, the MAPE decreased by 27.3%, and the determination coefficient increased by 2.8% in the dataset related to circular culverts compared to rectangular ones. The analysis of the outcomes from both datasets indicates that the proposed model exhibits a high level of capability and reliability, as the output for both training and testing data is nearly identical. However, it is important to note that there was a significant discrepancy in the results obtained for MAE and RMSE due to differences in the prototype scale and measuring units used in the two datasets.

6.2. Comparison of results with the standard ANFIS

A comparison was made between the standard ANFIS and ANFIS–TLBO to assess the effectiveness of the proposed models and evaluate the applied optimization technique (refer to Table 7). An analysis of the ANFIS–TLBO results indicated an increase in ANFIS efficiency, as illustrated in Figure 7. To ensure a precise comparison between the two models and mitigate the influence of data selection and model construction, identical conditions were employed for both models.

The analysis of the results reveals a noteworthy improvement in the ANFIS model's efficiency and prediction capabilities achieved through the optimization process. The ANFIS–TLBO model employs meticulously chosen configuration parameters, such as the influence radius, maximum iteration number, error objective, initiation step size, step size reduction rate, and increment rate for step size, to enhance the model's performance.

The analysis of the circular culverts dataset reveals a substantial increase of 30.2% in the coefficient of determination (R^2), pointing to a significant improvement in the model's ability to elucidate the variance in the data. This upsurge in R^2 signifies that the optimized ANFIS–TLBO model adeptly captures the underlying relationships between the input and output variables, resulting in more accurate predictions. Moreover, there is a noteworthy decrease of 46% in the RMSE, indicating a considerable reduction in the average prediction error of the model. This reduction in RMSE further underscores the enhanced prediction capabilities of the optimized model. Likewise, in the dataset for rectangular culverts, the optimized ANFIS–TLBO model exhibited a substantial 19.8% increase in R^2 and a noteworthy 25.6% decrease in RMSE. These improvements serve as an indication that the optimized model excels in capturing the complex relationships between the input and output variables within the dataset for rectangular culverts.

An important observation is that despite the satisfactory outcomes obtained by the standard ANFIS model during the training phase for both datasets, the testing phase produced suboptimal results. This indicates a potential occurrence of overfitting, where the standard ANFIS model becomes excessively tailored to the training data and fails to generalize effectively to unseen data. However, the proposed ANFIS–TLBO model exhibited nearly identical results in both the training and testing datasets, highlighting its improved reliability achieved through the optimization process.

A comparison of the convergence rates between the proposed ANFIS–TLBO model and the standard ANFIS model further substantiates the efficacy of the optimizations. The ANFIS–TLBO model displayed a superior convergence rate in both the datasets for circular culverts and rectangular culverts. This swifter convergence rate signifies that the optimized model can more efficiently and effectively attain the optimal solution.

It is worth noting that the standard ANFIS model achieved superior results for the cost function (training RMSE) in the circular culverts dataset. However, the model's validation efficiency using the test data were unsatisfactory due to excessive model training. This suggests that the standard ANFIS model may have been overfit to the training data, resulting in poor generalization to unseen data. The optimizations applied in the ANFIS–TLBO model help address this issue, resulting in improved performance in both the training and testing datasets. The comparison of the graphs presented in Figure 8 further illustrates the effectiveness of the optimizations implemented on the model. The optimizations have yielded a significant acceleration of the convergence rate, indicating that the ANFIS–TLBO model reaches the optimal solution more promptly and efficiently in comparison to the standard ANFIS model.

Table 7 | Comparative analysis of standard ANFIS and ANFIS–TLBO results for both datasets

		Train				Test			
Dataset	**Model**	R^2	**MAPE (%)**	**RMSE (mm)**	**MAE (mm)**	R^2	**MAPE (%)**	**RMSE (mm)**	**MAE (mm)**
Circular culverts	ANFIS	87.2	52.5	456	301	67.5	35.8	542	324
	ANFIS–TLBO	90.1	46.5	209	122	88.3	33.5	226	154
Rectangular culverts	ANFIS	86.3	65.3	51.2	32.3	71.3	91.8	54.2	33.8
	ANFIS–TLBO	87.5	33.8	31.4	22.5	82.5	25.9	30.7	25.2

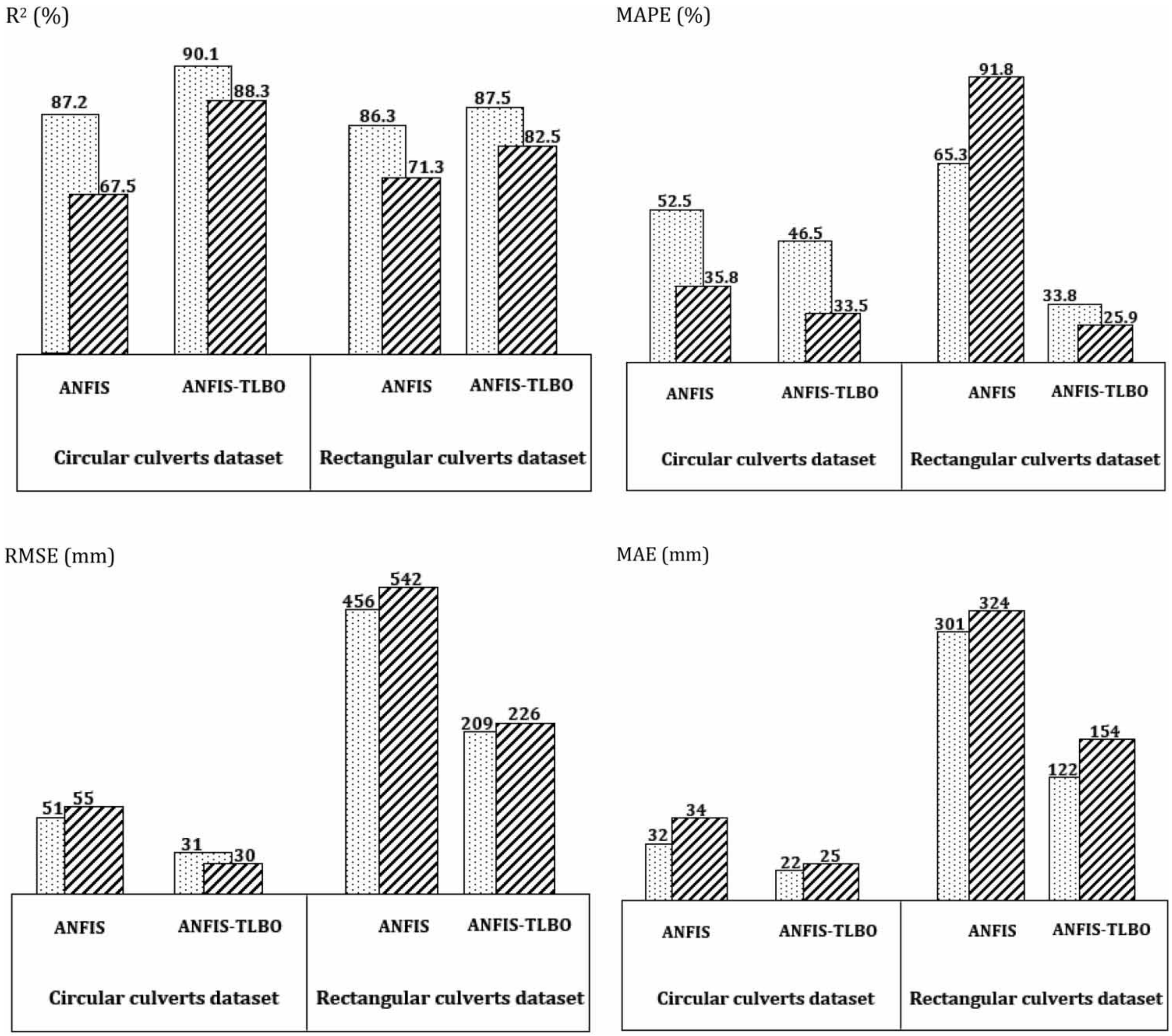

Figure 7 | Comparison of evaluation function results between ANFIS–TLBO and standard ANFIS.

The results unequivocally demonstrate that the optimization of the ANFIS model through the proposed ANFIS–TLBO configuration has yielded substantial improvements in both the efficiency and prediction capabilities of the model. The optimized model attained elevated coefficients of determination (R^2) and reduced RMSE in both the datasets for circular culverts and rectangular culverts. Furthermore, the ANFIS–TLBO model showcased a higher convergence rate and enhanced reliability when compared to the standard ANFIS model. Overall, these results highlight the efficacy of the optimizations in enhancing the performance of the ANFIS model for culvert prediction tasks.

6.3. Comparison of the results with empirical equations

The use of empirical equations is an important method for predicting scouring at culvert outlets. Various empirical relationships have been proposed to evaluate the maximum depth of scour at culvert exits. In this study, the obtained outcomes were compared with the most well-known empirical equations for circular outlets to assess the effectiveness of the proposed model; Figures 9 and 10. Similarly, several observations are made.

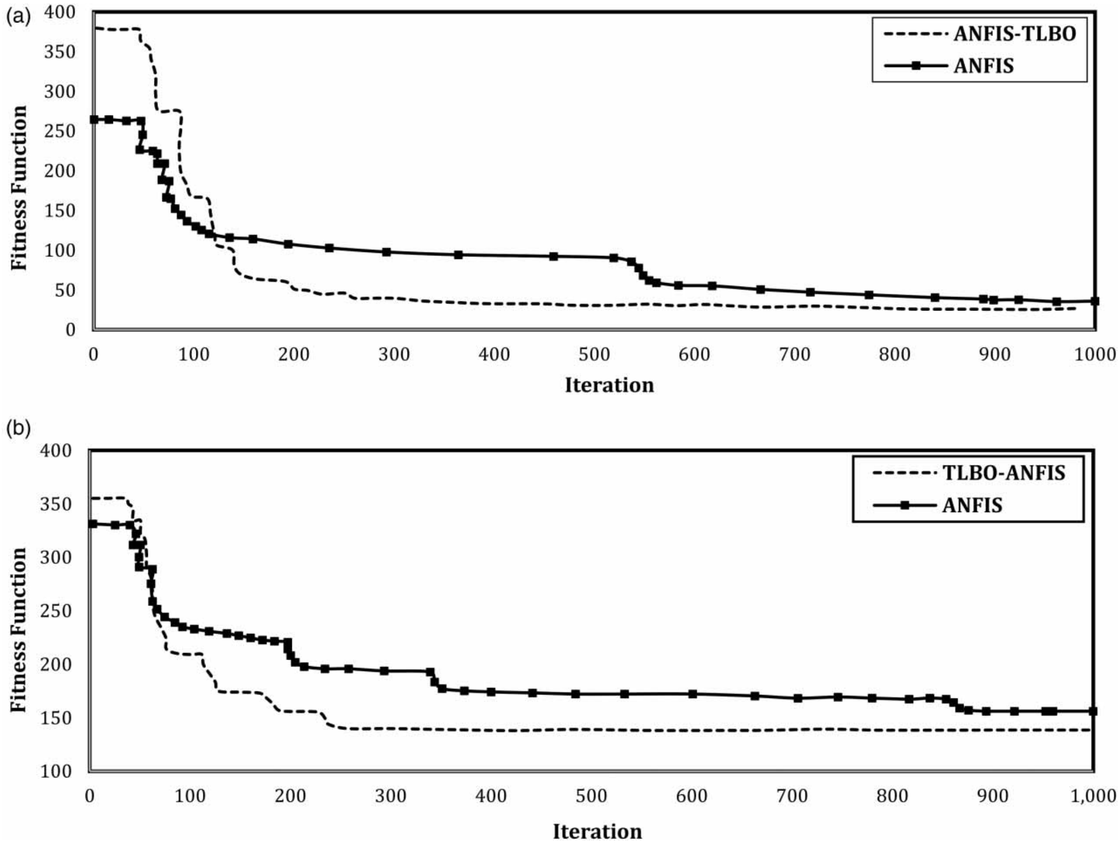

Figure 8 | Convergence history for the best testing fold in the dataset of (a) circular culverts and (b) rectangular culverts.

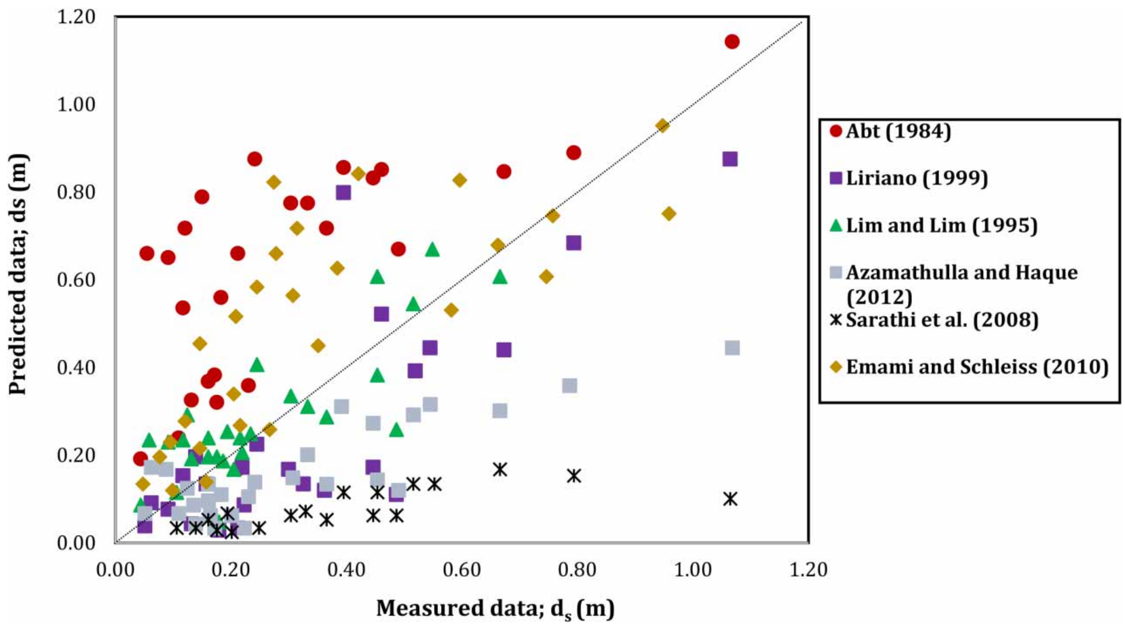

Figure 9 | Comparison of predicted and measured data for circular culverts using equation Group B.

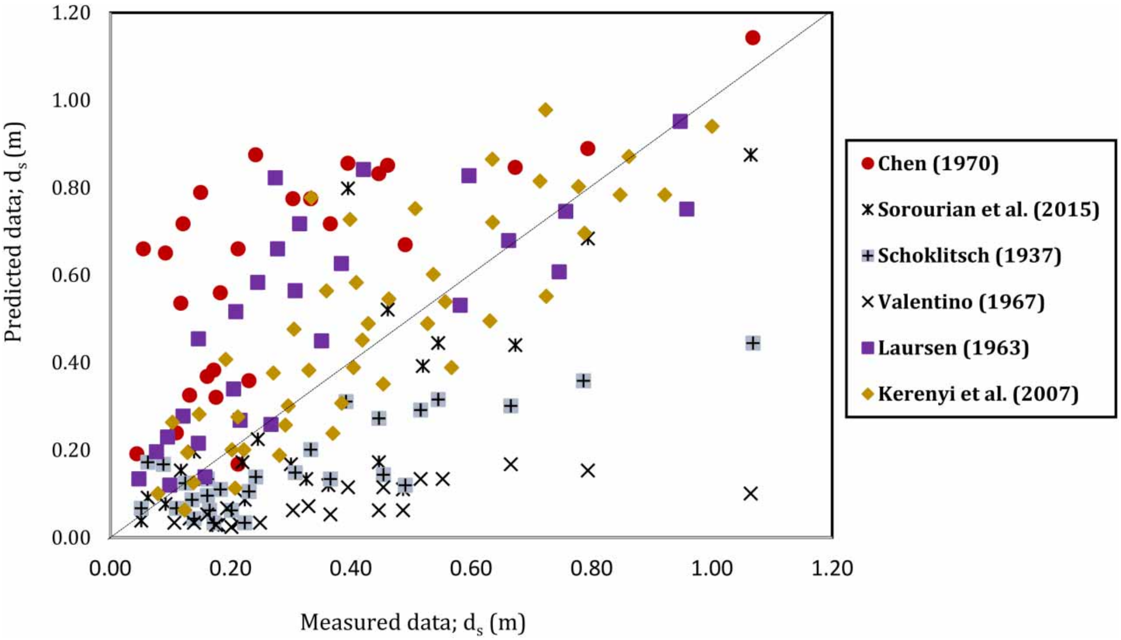

Figure 10 | Comparison of predicted and measured data for rectangular culverts using equation Group A.

The results obtained from the analysis of different equations for estimating the maximum depth of scour in circular culverts provide valuable insights into their performance and accuracy. It is evident from the figures and comparisons that not all equations yield equally reliable estimations.

The equation of Abt *et al.* (1985) displays a significant overestimation, with an average overestimation ratio of 80%. This indicates that the predicted values are consistently higher than the actual scour depth. On the other hand, Lim and Lim's equation (Lim & Lim 1995) demonstrates better performance, with an average over-prediction of 53%. While still overestimating, it provides a comparatively closer estimation of the actual scour depth.

Liriano's equation (Liriano 1999) and the equation of Azamathulla & Haque (2012) tend to overestimate the maximum scour depth, with only a few instances of underestimation. Liriano's equation, in particular, exhibits an average underestimation of 26%, indicating that it consistently predicts lower scour depths. However, it is worth mentioning that Liriano's equation performs better than Lim and Lim's equation in terms of accuracy, as it provides more accurate calculations on average, despite the underestimation. The equation of Sarathi *et al.* (2008) demonstrates an average underestimation of 22%, suggesting that it consistently predicts lower scour depths as well. In comparison to Liriano's equation (Liriano 1999), Sarathi's equation (Sarathi *et al.* 2008) performs better in terms of accuracy. The equation proposed by Azamathulla & Haque (2012) stands out as the most accurate among the equations analyzed. It provides the closest estimation to the actual maximum scour depth for circular culverts, as supported by the figure. This equation should be considered as a reliable tool for estimating scour depth in practical engineering applications.

It is important to note that Emami and Schleiss' equation (Emami & Schleiss 2010) tends to over-predict the maximum depth of scour. Therefore, caution must be exercised when utilizing this equation to ensure the structural safety of culverts. Further evaluation and refinement of this equation may be necessary to improve its accuracy.

In summary, the analysis of different equations for estimating the maximum depth of scour in circular culverts highlights the variation in their performance. While some equations tend to overestimate or underestimate, others provide more accurate estimations. The equation proposed by Azamathulla & Haque (2012) emerges as the most accurate among the evaluated equations. Nonetheless, it is crucial to consider the specific conditions and limitations of each equation and continue research efforts to improve their accuracy and reliability in practical engineering applications.

In some cases, some equations are originally developed based on envelope curves to guarantee the safety of predictions. The purpose of using envelope curves in these equations is to account for uncertainties and potential variations in the input parameters or conditions. By adopting a more conservative approach, engineers and researchers can ensure that the predicted values are within safe limits, even in worst-case scenarios. Predictions stemming from the use of envelope curves may lead to potential overdesign or unnecessary costs. Therefore, it is crucial to strike a balance between safety considerations and practical feasibility when applying these equations in engineering or decision-making processes. While equations based on envelope curves are valuable tools for ensuring safety, it is essential to be aware of their tendency to overestimate predictions. Evaluating the specific requirements and tradeoffs associated with each situation will help in making informed decisions regarding the use of these equations.

7. CONCLUSION

The research conducted underscores the significance of precise prediction of the maximum depth of scouring at culvert exits in order to guarantee appropriate culvert design. This study introduces a novel model employing the ANFIS algorithm and TLBO optimization method to estimate the maximum scour depth at both circular and rectangular culvert exits. The incorporation of TLBO into the ANFIS model significantly improved its accuracy in predicting scour depth. Experimental datasets were utilized to train and evaluate the proposed model. The model's predictive ability was assessed, and the effect of various parameters, such as culvert diameter and sediment size, on scouring depth was investigated.

The proposed model was then compared to standard ANFIS and other empirical equations to evaluate its performance. The results obtained from the five-fold cross-validation of the proposed model for both circular and rectangular culvert datasets demonstrated the efficacy of incorporating TLBO into the ANFIS. The R^2 coefficient increased, and the RMSE value decreased considerably when using TLBO–ANFIS. This indicates that the proposed model provides more accurate predictions of maximum scour depth compared to traditional ANFIS models. Furthermore, a comparison was made with existing empirical equations that have been suggested in the past to determine the maximum depth of scour. Thirteen equations were selected based on important parameters, and the accuracy of these equations was evaluated for both circular and rectangular culverts. The ANFIS–TLBO method outperformed the empirical equations, yielding the most optimal results for predicting the maximum scour depth at all culvert exits. In addition, a sensitivity analysis was conducted to examine the impact of specific parameters on scour depth anticipation. The results revealed that the culvert diameter (width) was the most influential parameter in determining scour depth. In conclusion, the developed ANFIS–TLBO model proves to be a highly effective approach for estimating the maximum scour depth at culvert exits. Its improved accuracy compared to standard ANFIS models and empirical equations makes it a valuable tool for engineers and designers involved in culvert design. By considering parameters such as culvert diameter and sediment size, the model provides reliable predictions and enhances the understanding of scouring phenomena. Further research and validation can be pursued to enhance the model's applicability and broaden its scope in the field of culvert design.

Overall, this study contributes to the advancement of knowledge in predicting scour depth at culvert exits and provides a practical and reliable tool for engineers in designing culverts that can withstand potential scouring effects. After performing this estimation, it is of utmost importance to give significant attention to reducing the scour depth at culvert outlets. This can be achieved by thoroughly evaluating new methods for effectively controlling the scouring downstream of culverts. One potentially effective method for reducing scour is the application of chemical materials as adhesive agents within the sediment bed. These chemical materials can help enhance the stability and cohesion of the sediment, thereby reducing the likelihood of scour occurrence.

DATA AVAILABILITY STATEMENT

All relevant data are included in the paper or its Supplementary Information.

CONFLICT OF INTEREST

The authors declare there is no conflict.

REFERENCES

Abdulelah Al-Sudani, Z., Salih, S. Q., Sharafati, A. & Yaseen, Z. M. 2019 Development of multivariate adaptive regression spline integrated with differential evolution model for streamflow simulation. *Journal of Hydrology* **573**, 1–12. https://doi.org/10.1016/j.jhydrol.2019.03.004.

Abida, H. & Townsend, R. D. 1991 Local scour downstream of box-culvert outlets. *Journal of Irrigation and Drainage Engineering* **117** (3), 425–440.

Abraham, A., 2005 Adaptation of fuzzy inference system using neural learning. In: *Fuzzy Systems Engineering. Studies in Fuzziness and Soft Computing*, Vol. 181 (Nedjah, N. & Macedo Mourelle, L. eds.). Springer, Berlin, Heidelberg.

Abt, S. R., Kloberdanz, R. L. & Mendoza, C. 1984 Unified culvert scour determination. *Journal of Hydraulic Engineering* **110** (10), 1475–1479.

Abt, S. R., Donnell, C. A., Ruff, J. F. & Doehring, F. K. 1985 Culvert slope effects on outlet scour. *Journal of Hydraulic Engineering* **111** (10), 1363–1367.

Ade, F. & Rajaratnam, N. 1998 Generalised study of erosion by circular horizontal turbulent jets. *Journal of Hydraulic Research* **36** (4), 613–636.

Aderibigbe, O. & Rajaratnam, N. 1998 Effect of sediment gradation on erosion by plane turbulent wall jets. *Journal of Hydraulic Engineering (ASCE)* **124** (10), 1034–1042.

Ali, K. H. M. & Lim, S. Y. 1986 Local scour caused by submerged wall jets. *Proceedings of the Institution of Civil Engineers* **81** (4), 607–645.

Azamathulla, H. M. & Ghani, A. A. 2010 ANFIS-based approach for predicting the scour depth at culvert outlets. *Journal of Pipeline Systems Engineering and Practice* . **2** (1), 35–40.

Azamathulla, H. M. & Haque, A. A. M. 2012 Prediction of scour depth at culvert outlets using gene-expression programming. *International Journal of Innovative Computing, Information and Control* **8** (7B), 5045–5054.

Azamathulla, H. M. & Haque, A. A. M. 2013 Knowledge extraction from trained neural network scour model at culvert outlets. *Neural Computing and Applications* **23** (7–8), 2137–2141.

Azamathulla, H. M., Deo, M. & Deolalikar, P. 2008 Alternative neural networks to estimate the scour below spillways. *Advanced in Engineering Software* **39** (8), 689–698.

Bohan, J. P. 1970 *Erosion and Riprap Requirements at Culvert and Storm-Drain Outlets*. Army Engineers Waterways Experiment Station, Vicksburg, MS, USA. Research report H-70-2, DTIC document.

Chen, Y. H. 1970 *Scour at Outlets of Box Culverts*. M.S. Thesis. Colorado State University, Fort Collins, Colorado.

Emami, S., Schleiss, A. J., 2010 Prediction of localized scour hole on natural mobile bed at culvert outlets. In: *Proceedings 5th International Conference on Scour and Erosion (ICSE-5), November 7–10, 2010, San Francisco, USA. Reston, Va* (Burns, S. E., Bhatia, S. K., Avila, C. M. C. & Hunt, B. E. eds.). American Society of Civil Engineers, San Francisco, CA, USA, pp. 844–853.

Ghorbani, M. A., Deo, R. C., Yaseen, Z. M. & Kashani, M. H. 2017 Pan evaporation prediction using a hybrid multilayer perceptron-firefly algorithm (MLP-FFA) model: Case study in North Iran. doi:10.1007/s00704-017-2244-0.

Hassanzadeh, H., Jafari-Bavil-Olyaei, A., Aalami, M. T. & Kardan, N. 2019 Experimental and numerical investigation of bridge pier scour estimation using ANFIS and teaching-learning-based optimization methods. *Engineering with Computers* **35**, 1103–1120.

Hu, J., Li, Y. & Chanson, H. 2022 Near-full-scale physical modeling and open-channel flow velocity in a fish-friendly culvert with full-height sidewall baffles. In: *Proc. 9th International Symposium on Hydraulic Structures ISHS2022*, 24–27 October, Roorkee, India, pp. 10.

Jang, J. S. R. 1993 ANFIS: Adaptive network based fuzzy inference system. *IEEE Transactions on Systems, Man, and Cybernetics* **23** (3), 665–685.

Ji, G., Wang, J., Ge, Y. & Liu, H. 2014 Urban water demand forecasting by LS-SVM with tuning based on elitist teaching-learning-based optimization. In: *Control and Decision Conference (2014 CCDC), the 26th Chinese*. IEEE, pp. 3997–4002.

Kerenyi, K., Jones, J. S. & Stein, S. 2007 *Bottomless Culvert Scour Study: Phase II Laboratory Report. FHWA-HRT-07-026.* Office of Engineering Research and Development, Federal Highway Administration, McLean, VA, p. 77.

Larry, M. 2017 *Healthy Culvert Make for Healthy Drinking Water*. Office of Communication, U.S. Forest Service, Washington DC, USA.

Laursen, E. M. 1963 An analysis of relief bridge scour. *ASCE Journal of Hydraulic Division* **89**, 93–118.

Li, Z., Harley, J. & Chanson, H. 2022 Physical modeling of pipe culverts to assist upstream fish Passage. *River Research and Applications* **38**, 319–322.

Lim, S. Y. 1995 Scour below unsubmerged full flowing culvert outlets. *Proceedings of the Institution of Civil Engineers Water Maritime and Energy* **112** (2), 136–149.

Lim, S. Y. & Lim, S. 1995 Scour below unsubmerged full-flowing culvert outlets. *Proceedings of the Institution of Civil Engineers Water Maritime and Energy* **112** (2), 136–149.

Liriano, S. L. 1999 *The Influence of Near bed Turbulent Flow Structures on Scour Hole Development at Pipe Culvert Outlets*. Doctoral dissertation. University of Hertfordshire, Hertfordshire, UK.

Liriano, S. L. & Dey, R. A. 2001 Prediction of scour depth at culvert outlets using neural networks. *Journal of Hydroinformatics* **3** (4), 231–238.

Liriano, S. L., Day, R. A. & White, W. R. 2002 Scour at culvert outlets as influenced by the turbulent flow structure. *Journal of Hydraulic Research* **40** (3), 367–376.

Maier, H. R., Kapelan, Z., Kasprzyk, J., Kollat, J., Matott, L. S., Cunha, M. C., Dandy, G. C., Gibbs, M. S., Keedwell, E., Marchi, A., Ostfeld, A. & Savic, A. 2014 Evolutionary algorithms and other metaheuristics in water resources: Current status, research challenges and future directions. *Environmental Modelling & Software* **62**, 271–299. https://doi.org/10.1016/j.envsoft.2014.09.013.

Najafzadeh, M. 2015 Neurofuzzy-based GMDH-PSO to predict maximum scour depth at equilibrium at culvert outlets. *Journal of Pipeline Systems Engineering and Practice* **7** (1), 06015001.

Najafzadeh, M. 2016 Neurofuzzy-Based GMDH-PSO to predict maximum scour depth at equilibrium at culvert outlets. *Journal of Pipeline Systems Engineering and Practice* **7** (1), 1–5.

Najafzadeh, M. & Kargar, A. R. 2019 Gene-expression programming, evolutionary polynomial regression, and model tree to evaluate local scour depth at culvert outlets. *Journal of Pipeline Systems Engineering and Practice* **10** (3), 04019013.

Opie, T. P. 1968 *Scour at Culvert Outlets*. Colorado State University, Colorado, America.

Rajaratnam, N. 1981 Erosion by plane turbulent wall jets. *Journal of Hydraulic Research* **19** (4), 339–358.

Rajaratnam, N. & Berry, B. 1977 Erosion by circular turbulent wall jets. *Journal of Hydraulic Research* **15** (3), 277–289.

Rajaratnam, N. & MacDougall, R. K. 1983 Erosion by plane wall jets with minimum tailwater. *Journal of Hydraulic Engineering* **109** (7), 1061–1064.

Rao, R. V., Savsani, V. J. & Vakharia, D. 2011 Teaching-learning-based optimization: A novel method for constrained mechanical design optimization problems. *Computer-Aided Design* **43** (3), 303–315.

Roy, P. K., Sur, A. & Pradhan, D. K. 2013 Optimal short-term hydrothermal scheduling using quasi-oppositional teaching learning based optimization. *Engineering Application of Artificial Intelligence* **26** (10), 2516–2524.

Ruff, J. F., Abt, S. R., Mendoza, C., Shaikh, A. & Kloberdanz, R. 1982 *Scour at Culvert Outlets in Mixed bed Materials (No. FHWA/RD-82/011). United States*. Federal Highway Administration. Office of Research and Development, Washington, DC, USA.

Sarathi, P., Faruque, M. A. A. & Balachandar, R. 2008 Influence of tailwater depth, sediment size and densimetric Froude number on scour by submerged square wall jets. *Journal of Hydraulic Research* **46** (2), 158–175.

Schoklitsch, A. 1937 *Prevention of Scour and Energy Dissipation*. Translated by Edward, F. U.S. Department of the Interior, Bureau of Reclamation, United States, p. 172.

Sharafati, A., Khosravi, K., Khosravinia, P., Ahmed, K., Salman, S. A., Mundher, Z. & Shamsuddin, Y. 2019 The potential of novel data mining models for global solar radiation prediction. *Journal of Environmental Science and Technology* https://doi.org/10.1007/s13762-019-02344-0.

Sharafati, A., Tafarojnoruz, A., Motta, D. & Yaseen, Z. M. 2020a Application of nature-inspired optimization algorithms to ANFIS model to predict wave-induced scour depth around pipelines. *Journal of Hydroinformatics* **22** (6), 1425–1451. https://doi.org/10.2166/hydro.2020.184.

Sharafati, A., Tafarojnoruz, A. & Yaseen, Z. M. 2020b New stochastic modeling strategy on the prediction enhancement of pier scour depth in cohesive bed materials. *Journal of Hydroinformatics* **22** (3), 457–472. https://doi.org/10.2166/hydro.2020.047.

Sharafati, A., Tafarojnoruz, A., Shourian, M. & Yaseen, Z. M. 2020c Simulation of the depth scouring downstream sluice gate: the validation of newly developed data-intelligent models. *Journal of Hydro-Environment Research* **29**, 20–30. https://doi.org/10.1016/j.jher.2019.11.002.

Sorourian, S., Keshavarzi, A., Ball, J. & Samali, B. 2014 Blockage effects on scouring downstream of box culverts under unsteady flow. *Australasian Journal of Water Resources* **18** (2), 180–190.

Sorourian, S. 2015 Turbulent flow characteristics at the outlet of partially blocked box culverts. *E-proceedings of the 36th IAHR World Congress*, 28 June–3 July, The International Association for Hydro-Environment Engineering and Research (IAHR), The Hague, The Netherlands.

Sorourian, S., Keshavarzi, A. & Ball, J. E. 2016 Scour at partially blocked box-culverts under steady flow. *Proceedings of the Institution of Civil Engineers Water Maritime and Energy* **169** (WM6), 247–259.

Toğan, V. 2012 Design of planar steel frames using teaching–learning based optimization. *Engineering Structures* **34**, 225–232.

Valentin, F. 1967 Considerations concerning scour in the case of flow under gates. *Proceedings of the Twelfth Congress of the IAHR*, vol.3, Colorado State University, Fort Collins, Colorado.

Yaseen, Z. M., El-shafie, A., Jaafar, O., Afan, H. A. & Sayl, K. N. 2015 Artificial intelligence based models for stream-flow forecasting: 2000–2015. *Journal of Hydrology* **530**, 829–844. https://doi.org/10.1016/j.jhydrol.2015.10.038.

Yaseen, Z. M., Awadh, S. M., Sharafati, A. & Shahid, S. 2018a Complementary data-intelligence model for river flow simulation. *Journal of Hydrology* **567**. https://doi.org/10.1016/j.jhydrol.2018.10.020.

Yaseen, Z. M., Ehteram, M., Sharafati, A., Shahid, S., Al-Ansari, N. & El-Shafie, A. 2018b The integration of nature-inspired algorithms with Least Square Support Vector regression models: Application to modeling river dissolved oxygen concentration. *Water* **10**. https://doi.org/10.3390/w10091124.

Zhang, R. & Wu, P. 2021 The investigation of shape factors in determining scour depth at culvert outlets. *ISH Journal of Hydraulic Engineering* **27** (7), 1–7.

First received 10 March 2024; accepted in revised form 16 July 2024. Available online 7 August 2024